NEW PASSENGER RESTRAINTS WITH ADAPTIVITY TO OCCUPANT SIZE, SEATING POSITIONS AND CRASH SCENARIOS THROUGH PAIRED ATD-HM STUDY

Jay Zhao
Pareed Kumar Jakkamsetti
Maika Katagiri
Sungwoo Lee
Joyson Safety Systems
United States,

Paper Number 19-0322

ABSTRACT

This study was undertaken to develop new passenger side Advanced Adaptive Restraint Systems to better protect automobile passenger occupants from serious injuries in frontal and oblique motor vehicle crashes.

New concept designs of a passenger airbag and a knee airbag, each with controllable dual-volume and tunable vents, were developed. A new advanced adaptive restraint system, integrated with such developed passenger airbag, knee airbag and an updated seatbelt system consisting of a switchable dual-load limiter retractor with shoulder and lap pretensioners, was optimized to achieve good performance for all the fourteen load cases defined in this study.

The fourteen load cases represent various real-world crash scenarios comprising passengers of three body sizes seated at different seating positions (the small-size female at full-forward, mid-track, and full-rearward, the mid-size and large-size males at mid-track and full-rearward) under a "hard" pulses representing the 35mph full frontal and frontal oblique crashes of a sub-compact passenger car. The system performances were evaluated with the two sets of occupant injury assessment tools: 1) the Anthropomorphic Test Devices (ATDs) of the three body sizes (the Hybrid-III 5th%ile female dummy, the THOR 50th%ile mid-size male dummy and the Hybrid-III 95th%ile large-size male dummy) with the injury risk functions used in current regulatory lab tests, and 2) the full body Human Models (HMs) of the three body sizes (the 5th%ile female model F05-O v3.1, the 50th%ile male model M50-O v4.5 and the 95th%ile male model M95-O v1.2) developed by Global Human Body Model Consortium (GHBMC)) with the published injury risk functions derived from the Postmortem Human Subject (PMHS) tests. For each load case, four passenger side sled system models were developed, paired with the ATD and the HM of the same size, and for the current production restraints (baseline) as well as the new restraint designs. The injury risks of the occupant body regions and combined injury risks (referred to "Occupant Injury Measures") were estimated with both ATDs and HMs.

The new adaptive restraint system design was developed through individualized optimization for all the fourteen cases in multiple iterative steps. Firstly, the new concept designs were made at the component level, evaluated using two validated ATD sled test models simulating the two load cases (5th%ile female at full-forward position and 50th%ile male in full-rearward position). Secondly, the new advanced adaptive restraint system was optimized with the ATDs in seven successive steps, obtained the optimal restraint design parameters set for each load case. And finally, the optimal adaptive restraint configuration for each case was verified with the HMs sled models. Hundreds of the sled simulations were performed in such processes.

The results demonstrated that the new adaptive passenger restraint system design has more versatile adaptivity and improved performances for all the considered load cases than the baseline restraints. The benefits for the occupant injury risks reduction vary case by case, within 12%-79% margin estimated with the ATDs and 8%-66% with the HMs.

INTRODUCTION

Since their introduction, restraint system technologies such as air bags and seat belts have been effective at mitigating injuries and fatalities associated with motor vehicle accidents. Over the past 40 years, there has been a general downward trend in traffic fatalities in the United State. Still, in 2017, there were 37,133 people killed in

motor vehicle traffic crashes in U.S. roadways ("NHTSA Traffic Safety Facts", DOT HS 812 603, October 2018). As such, the industry continues its efforts to improve restraint system effectiveness by adding new field relvant tests and adjusting the injury risk values to achieve higher rating.

In the past, passive restraint devices were designed as "one size fits all"— the restraint system performance in frontal crashes was optimized with one ATD size in one "standard" seating postion in a lab crash test. In the current enhanced regulatetory lab tests, two ATDs (representing 5th%ile female and 50th%ile male) at one seating positon each were deployed for a restraint system design performance evaluation. In the real world, however, occupant crash induced injuries occur to a large and highly variable population [Stewart C. Wang et al., 2016]. The injury severity and patterns are highly affected by occupants' demographic variables such as age, gender and size (height and weight), and morphomic variables such as BMI, body shape geometry, bone mineral density (HU), fat distribution etc. as well as crash variables such as seating position/posture, vehicle crash severity, and crash modes. A earlier study on CIREN & 1995-2005 NASS/CDS filed data [Bulger et al., 2005] concluded that occupants with fully reclined seat positions suffered higher real-world crash induced fatality rate. Other studies found that variability in occupant posture state resulted in maximum statistical dispersion in overall injury [Bose, et al., 2008], [Gaewsky J., 2015]. Therefore, improving occupant protection requires that the effectiveness of restraint devices be consistent across a wide range of these variables. Adaptive restraint systems will be needed to optimally protect an increasingly vulnerable occupant population in various real-world crashes.

To quantify the potential benefits of the "Adaptive Restraint Systems", the National Highway Traffic Safety Administration (NHTSA) sponsored the Advanced Adaptive Restraints Program (AARP) during 2014-2016, in which we investigated the opportunity to reduce injury to the driver and front right occupants by adapting the restraint system to three occupant sizes (5th%ile female represented by the Hybrid-III 5F dummy, 50th%ile male by the THOR-50M, and 95th%ile male by the Hybrid-III 95M dummy), four seating positions (full-forward, mid-track, rear, full-rear) and four postures (nominal, forward, outboard, inboard leaning), and two crash types (frontal & 15^{o} oblique) at two crash severities (35mph "hard" pulse and "soft" pulse) using a fully-functional prototype Advanced Adaptive Restraint System (referred to ARS1 in this study) [Cyliax et al. 2015]. The considered seating positions could be classified as two kinds: "In-Position (IP)" for the Federal Motor Vehicle Safety Standards (FMVSS) 208 defined or nominal positions, and "Out-Of-Position" (OOP) for those non-nominal or not defined in FMVSS 208. A sled evaluation matrix consisting of thirteen In-Position seated ATD sled tests and eleven Out-Of-Position tests was performed. For each load case, the restraint system performance was quantified by calculating the Occupant Injury Measure (OIM), which predicts the risk of injury as estimated by the Abbreviated Injury Scale (AIS) 3+. The OIM was calculated using the measures of head injury (Head Injury Criterion (HIC15)) and Brain Injury Criterion (BrIC)), neck injury (Neck Injury Criterion (NIJ)), chest injury (Chest Deflection (ChD)), and lower extremity injury (femur force) either measured or calculated for each test. Effectiveness of the tested adaptive restraint system over the baseline (current production restraints) was estimated from the study [Cyliax et al. 2015]. It showed that for the thirteen In-Position load cases, a reduced injury risk was achieved eleven of the front right passenger side load cases (ranging from 11% to 52% improvement). For the eleven Out-Of-Position load cases, however, a reduced risk of injury was achieved only in four of the front right passenger side load cases (1% to 20% improvement). Futher improvement of the ARS1 performance was desired especially for those Out-Of-Position seated occupants.

Our analysis of the AARP sled test data [Zhao et al., 2017] indicated that the injury risks for the occupants in some Out-of-Positions cases could be higher than those seated in the nominal position. In other words, the nominal seating positions defined in FMVSS 208 could not be the worst cases. The identified worst cases from the AARP study were: 1) the full-rearward seated mid-size and large-size males with higher injury risks of the body regions of chest, knee-thigh-hip and lower extremities; 2) The full-forward seated small-size female with higher injuries of the head and lower extremities; and 3) the small-size female or a mid-size male in the mid-track position at inboard leaning posture with higher injury risks of the head, neck and thorax under the left oblique crash. Another observation from the AARP study was that the Hybrid-III 95th%ile dummy had lower OIMs than the THOR 50th%ile male dummy across all the load cases. However, our analysis with the GHBMC human body models showed that a large size male could suffer higher injury risks than the mid-sized male at same position. It indicated that biofidelty of the Hybrid-III 95th%ile dummy is questionable. Evaluation of effectiveness of adaptive restraints requires more reliable biofidelic tools and evaluation methods than those used in current regulatory lab tests, especially for the larger-size occupants.

In the past decades new technologies of human body modeling have advanced. With NHTSA's support, GHBMC has been developing a series of human occupant models including detailed and simplified 5th%ile female, 50th%ile and 95th%ile males occupant models. These models have been validated at some extent at tissue, component and full body levels. These human models have high potential to be used as a virtual test tools representing real-world human occupants to assess the crash-induced injury risks. Evalution of the restraint performance could be made for both ATDs and HMs. Injury measures could be verifiable experimentally with ATDs; and the occupant injury risks could be estimated more realistically, especially for a large-size heavy occupant group, with HMs. In this study we deployed the detailed human models as supplemental injury assessment tools.

Considering all the facts and thoughts explained above, we were motivated to develop a new approach to design, evaluate and optimize adaptive restraints performance with paired ATD and HM sled test simulation models.

The objectives of this study were:

1) to develop new concept designs of adaptive restraints with good adaptivity and effectiveness for multiple load cases considering variations of the occupant sizes (height and weight), the seating positions and the crash modes at the severe ("hard") AARP 35mph crash pulse,
2) to develop a new methodology to evaluate and optimize the restraint system performance using both ATDs and HMs of three body sizes (5th%ile female, 50th%ile male and 95th%ile male),
3) to identify potential benefits of the new passenger adaptive restraint system.

METHODS

In this study, we focused on the passenger or right hand side occupants of vehicle first row. The development of new concept designs of adaptive restraints was executed in the multiple steps explained below.

ATD Sled System Models Validation

This computational study requires well validated sled test system models as good bases. For the model validation, we used a set of experimental data from the ATD sled tests performed in AARP. As listed in Table 1, thirteen sled tests were modeled, including the three sizes of ATDs (Hybrid-III 5th%ile female dummy, the 50th%ile Metric THOR dummy, and the Hybrid-III 95th%ile male dummy), the three seating positions (most Out-of-Position), and with both tested baseline and adaptive restraints.

Table 1.
The validation matrix for the passenger ATD sled models and the model correlation quality assessment summary

ATD	Case No	Pulse	Posture	Seat Position	Restraints	Kinematics Rating score	CORA Rating score	IR Rating Score
HB3-F05	1A	Hard 0°	Nominal	Full forward	Baseline	Good	0.64	0.02
	1C	Hard 0°	Nominal	Full forward	ARS1	Good	0.68	0.04
	2A	Hard15°	Nominal	Full forward	Baseline	Good	0.71	-0.01
	2C	Hard15°	Nominal	Full forward	ARS1	Good	0.70	-0.03
	5A	Hard 0°	Nominal	Full rear	Baseline	Good	0.60	0.10
	5C	Hard 0°	Nominal	Full rear	ARS1	Good	0.67	0.07
THOR-M50	7A	Hard 0°	Nominal	Mid-track	Baseline	Good	0.63	-0.09
	7C	Hard 0°	Nominal	Mid-track	ARS1	Good	0.71	0.02

	8A	Hard15	Nominal	Mid-track	Baseline	Good	0.66	-0.10
	9A	Hard 0°	Nominal	Full rear	Baseline	Good	0.66	0.05
	9C	Hard 0°	Nominal	Full rear	ARS1	Good	0.64	-0.06
HB3-M95	15A	Soft 0°	Forward	Mid-Track	Baseline	Good	0.56	0.02
	16A	Hard15	Nominal	Rear	Baseline	Fair	0.61	0.02

For each case in Table 1, correlation of the ATD sled test model with the test data was performed. The model correlation quality was assessed with the following method.

Three criteria or rating scores were calculated for each case in Table 1: 1) Kinematics Correlation Rating Score (from 1 to 5) by comparing snapshots the simulation and the test video at every 5msec during 0-120 msec; 2) CORA Rating Score for correlating the simulation and the test of the fifteen time-history curves essential for the ATD injury measures calculation; 3) Injury Risk Correlation Rating Score defined as the difference of the injury risks between the model predicted and the test, i.e., $IR = OIM_{model} - OIM_{test}$).

Table 1 summarizes the three rating scores for all the validation cases. A detailed model correlation for the injury risks between the calculated from the model and the test was shown in Figure A-1 in Appendix-A. Overall, good correlations were achieved for all the cases.

Load Cases and ATD-HM Paired Sled Models

Fourteen load cases as shown in Table 2 were defined for design and evaluation of new adaptive restraint systems. The conditions in each case varied with the occupant sizes, the seating positions, and the crash modes (represneted by the two sled angles). The "hard pulse", as shown in Figure B-1 in Appendix-B, represented a 35mph crash of a sub-compact car. The 0 degree sled represents the full frontal crashes, and the left 15 degree angled sled test simulates the oblique crashes.

Table 2.
Load cases for design and evaluation of new adaptive restraint systems

Occu. Size \Seating Position	Full-Forward (FF)	Mid-Track Position (MP)	Full-Rearwad (FR)
AF05	Case 1--0 deg "hard" pulse	Case 3--0 deg "hard" pulse	Case 5--0 deg "hard" pulse
	Case 2--15 deg "hard" pulse	Case 4--15 deg "hard" pulse	Case 6--15 deg "hard" pulse
AM50	NA	Case 7--0 deg "hard" pulse	Case 9--0 deg "hard" pulse
		Case 8--15 deg "hard" pulse	Case 10--15 deg "hard" pulse
AM95	NA	Case 11--0 deg "hard" pulse	Case 13--0 deg "hard" pulse
		Case 12--15 deg "hard" pulse	Case 14--15 deg "hard" pulse

For each case in Table 2, we built four sled models classified as A—ATD with the baseline restraints, B—human model (HM) with the baseline restraints, E— ATD with the new adaptive restraints, and F—HM with the new adaptive restraints. A complete list of all the sled test models is in Table B-1 in Appendix B.

Among the A- class sled models, the five model cases (1A, 2A, 5A, 7A, 9A) were the same validated cases in Table 1. For the other small-size female and mid-size male cases, each case model was built based on the validated case with similar conditions by only updating one system variable (such as the seating position or the pulse). For the large-size male cases, the case models were built from the validated cases 16A.

Each E- class sled model was built based on its partner of A- model by only replacing the baseline with the new designed adaptive restraints explained in the next section.

The class B- or F- class sled models were re-constructed from its ATD partner model by replacing it with the HM. The seatbelt route and seat cushion profiles were then adjusted to fit the HM body. It was noticed that even for the same body size the HM has somewhat different body shape and height than his/her partner of the ATD. To position the HM to the ATD as close as possible, the key body positioning measures, such as the HIP CG coordinates, the body reclined angle, the angles of upper and lower extremities, were kept as similar to partner ATD.

In total, fifty-six sled models were created for the fourteen load cases.

New Adaptive Restraints Design

New concept designs of adaptive restraints were developed based on the main requirement to make the system performances for all the load cases defined in Table 2 better than the baseline restraint. In addition, consideration for the components production feasibility was also kept in mind.

The component design of a new adaptive passenger airbag (PAB) was based on new concepts of adaptivity having adjustable dual-volume (large and small) and vents (discrete vents plus an active vent). Several PAB cushion designs with different shapes having such adaptivity were modeled. An inflator was selected and evaluated to fill the PAB cushion to the targeted volumes. The larger volume cushion coverage, stiffness and performance was evaluated with the load Case 9 (the 50^{th}%ile THOR dummy at full-rearward position at 0 deg hard pulse), while the smaller volume cushion coverage, stiffness and performance was evaluated with the load Case 1 (the 5^{th}%ile female dummy at full-rearward position at 0 deg hard pulse). Dozens of the ATD sled simulations for Case 1 and Case 9 were performed. The "best" performed PAB cushion was selected from this process for next design parameters optimization at system level.

New knee airbag (KAB) cushion designs were made with the similar idea for adaptivity as the PAB. Change of the deployed cushion volume was realized by changing the depth while keeping the coverage area about the same. An active vent was also introduced to make the cushion stiffness adjustable. A new design of KAB module with such adaptivity features was also evaluated with the simulations of Case 1 and Case 9. The "best" performer of the KAB concept design was identified for next design parameters optimization at system level.

The seatbelt system was upgraded from the system used in AARP. The same shoulder retractor with the switchable dual-load limiter and the pretensioner was used. Such a seatbelt model was further validated in the five sled cases in Table 1 (1C, 2C, 5C, 7C, 9C). Then a validated lap pretensioner model was added. Thus, the integrated new seatbelt system consists of the dual-pretensioner (shoulder and lap) and the dual-load limiter retractor with switchable loads.

The new passenger adaptive restraint system integrated the newly designed PAB, KAB and seatbelt components. The next step was to determine optimal set of restraint system design parameters for each load case through the optimization process at the system level as explained below.

System Performance Optimization

The system performance optimization was to determine a unique set of restraint system parameters for each load case such that the adaptive restraints enable optimal functionality for reducing the occupant injury risks for all the considered crash conditions.

Table C-1 summarizes the adaptive restraint system design parameters and the classification. As shown, there are eighteen design parameters, which can be classified into two types: non-programmable and programmable in the circuit board control units. The non-programmable or non-controllable parameters were those fixed in the restraint device design (such as a vent size), while the programmable parameters were those controllable inputs for the squibs (such as a time-to-fire).

Since a full scale optimization considering the seventeen design variables and the fourteen load cases is practically not doable, we developed a simplified process performing individualized optimization case by case iteratively. The work flow chart of such an optimization process is shown in Figure 1.

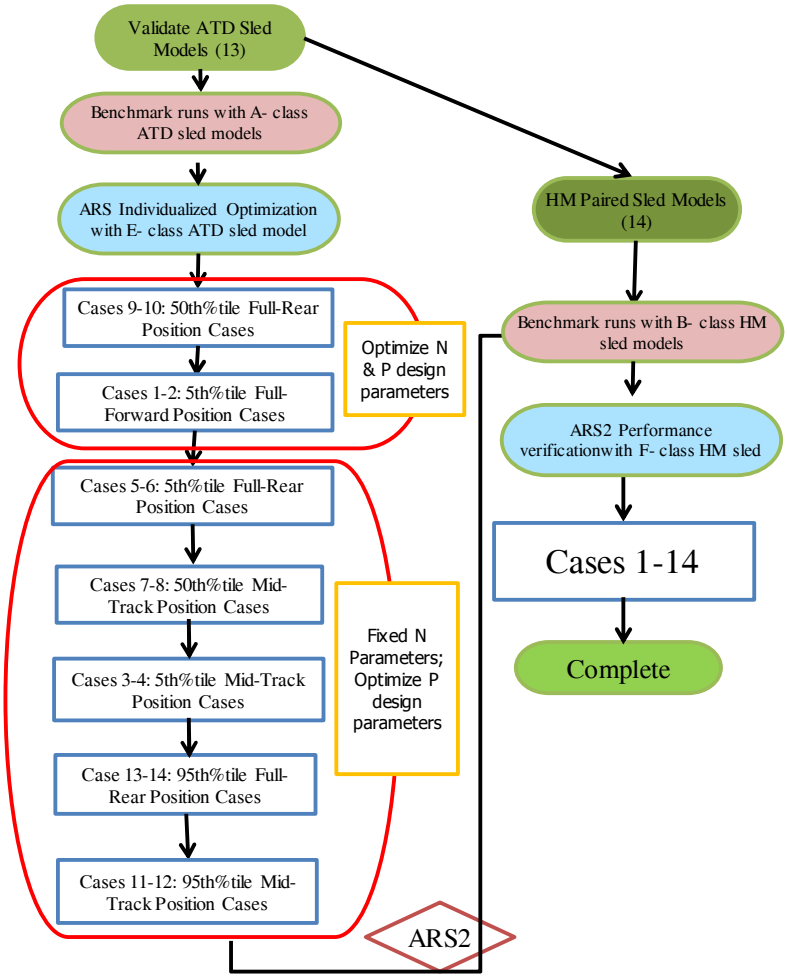

***Figure 1*. The work flow chart of the adaptive restraint optimization process**

The optimization for the new adaptive restraint systems was performed in two cycles: ATDs and HMs. The ATDs cycle was performing the individualized optimization for all the fourteen load cases with the E- class ATD sled models. The adaptive restraint systems with optimal system parameters for each load case were obtained from this cycle (referred to "ARS2" in this paper). The HMs cycle verified the ARS2 system performance using the F- class HM sled models with the injury risks assessment based on the OIMs outputted from the HMs.

In the ATDs cycle, the individualized optimization was executed at seven successive steps for all the load cases in the order shown in Figure 1. At each step, we run iteratively the DOE (Design-of-Experiment) matrices until an optimal set of the system design parameters were found out. In the first two steps for Cases 9-10 ad 1-2, the non-programmable and programmable design parameters were optimized simultaneously, and at the end those optimal non-programmable parameters were determined. While in the last five steps, only those programmable system design parameters were included in the DOE matrices for the optimization. In this way, the total number of DOE iterations was reduced significantly. The ARS2 system configuration with optimal design parameters for each load case was defined in this cycle.

In the HMs cycle, the same ARS2 system configuration from the ATD optimization was implemented into the F- class HM sled model for each load case. The ARS2 benefits were assessed with the HMs explained below.

Injury Risks Calculation and Benefit Assessment

The Occupant Injury Measure (OIM_{AIS3+}^{ATD}) for the AIS 3+ injury risk estimated from the ATDs was calculated by (1)

$$OIM_{AIS3+}^{ATD} = 1 - (1 - P_{HIC}) * (1 - P_{BrIC}) * \left(1 - Max(P_{NIJ}, P_{NeckFz+}, P_{NeckFz-})\right) * (1 - P_{ChCD}) * (1 - P_{FemurF})$$

(Equation 1)

where P_{HIC}, P_{BrIC}, $P_{NIJ}, P_{NeckFz+}, P_{NeckFz-}$, P_{ChCD}, P_{FemurF} are the AIS 3+ injury probabilities calculated with the measures of Head Injury Criterion (HIC15) and Brain Injury Criterion (BrIC), Neck Injury Criterion (NIJ) and Neck Extension and Compression Forces, Chest Deflections, and Femur Force, respectively. Table D-1 in Appendix-D summarizes the formulas for these probabilities and references for the three ATD sizes: the Hybrid-III 5th%ile small-size female dummy, the 50th%ile mid-size male THOR and the Hybrid-III 95th%ile large size male dummy.

The Occupant Injury Measure (OIM_{AIS3+}^{HM}) for the AIS 3+ injury risk estimated from the HMs was calculated by (2)

$$OIM_{AIS3+}^{HM} = 1 - (1 - p_{HIC}) * (1 - p_{BrIC}) * \left(1 - Max(p_{NeckFz+}, p_{NeckFz-})\right) * (1 - p_{ChCD}) * (1 - p_{FemurF})$$

(Equation 2)

where p_{HIC}, p_{BrIC}, $p_{NeckFz+}, p_{NeckFz-}$, p_{ChCD}, p_{FemurF} are the AIS 3+ injury probabilities calculated with the measures of Head Injury Criterion (HIC15) and Brain Injury Criterion (BrIC), Neck Extension and Compression Forces, Chest Deflections, and Femur Force, respectively. Table D-2 in Appendix-D summarizes the formulas for these probabilities and references for the three HM sizes: the 5th%ile small-size female HM, the 50th%ile mid-size male HM and the 95th%ile large size male HM. It is noted that the chest deflections were defined and outputted at the five locations at the thorax: the center of the sternum, and the upper left and right, and the lower left and right. The last four locations are same as the THOR dummy for comparison. The chest deflection at the sternum center was used for calculating the injury risk of the thorax region.

The benefit of new adaptive restraints was estimated by the percentage of reduction of the OIM from the ARS2 over the OIM from the baseline restraints.

To establish a benchmark for comparison, the ATD sled simulations for the baseline restraints (with A- class models) were performed and the results were processed. Also, the HM sled simulations for the baseline restraints (with E- class models) were performed.

RESULTS

Occupant Injury Measures from ATDs

Figure 2 compares the Occupant Injury Measures for the AIS 3+ injury risks between the optimal adaptive restraints (ARS2) and the baseline restraints for the fourteen load cases. The calculations were based on the body injury measures outputted from the ATDs as listed in Table E-1 in Appendix E. The ATD study showed that the ARS2 had the lower OIMs than the baseline across all the load cases. The percentages of the AIS 3+ injury measure reduction over the baseline were in the range of 12%-79%. For all the fourteen load cases, there were no case with the baseline restraints in which the OIM was less than 20%. The adaptive restraint system brought down the OIMs of two cases below 20%.

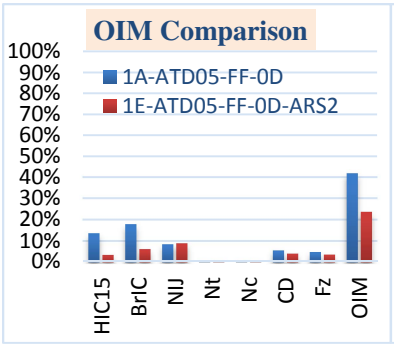

(i) Case 1E vs. 1A

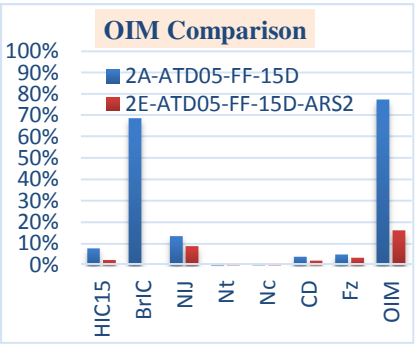

(ii) Case 2E vs. 2A

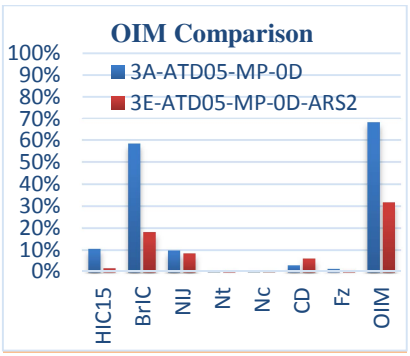

(iii) Case 3E vs. 3A

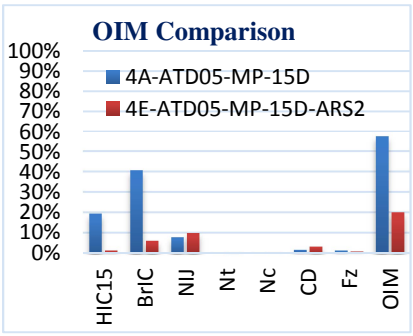

(i) Case 4E vs. 4A

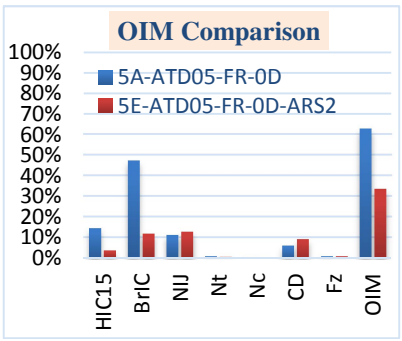

(ii) Case 5E vs. 5A

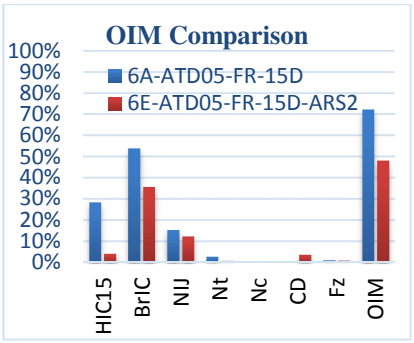

(iii) Case 6E vs. 6A

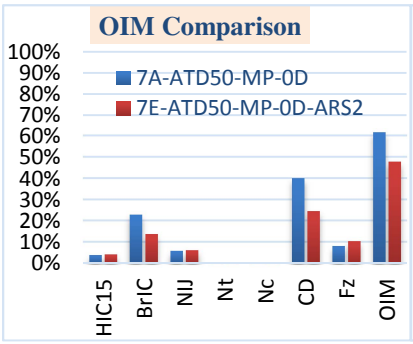

(i) Case 7E vs. 7A

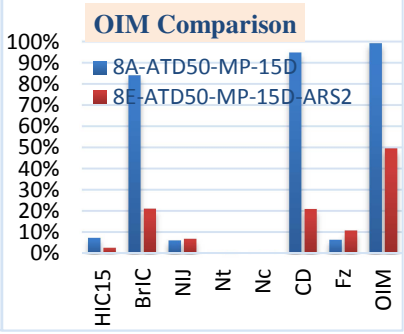

(ii) Case 8E vs. 8A

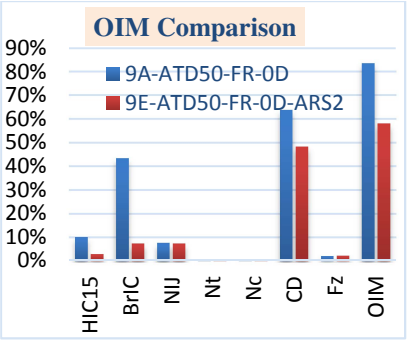

(iii) Case 9E vs. 9A

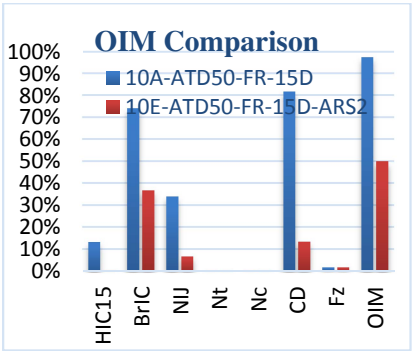

(i) Case 10E vs. 10A

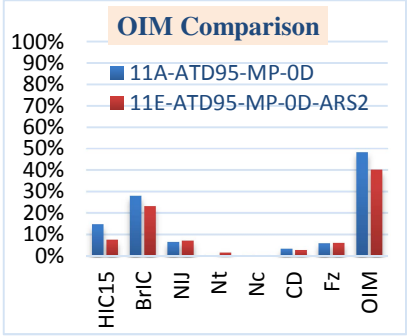

(ii) Case 11E vs. 11A

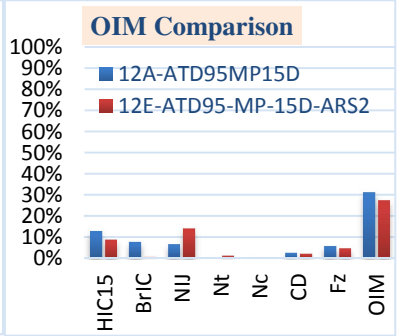

(iii) Case 12E vs. 12A

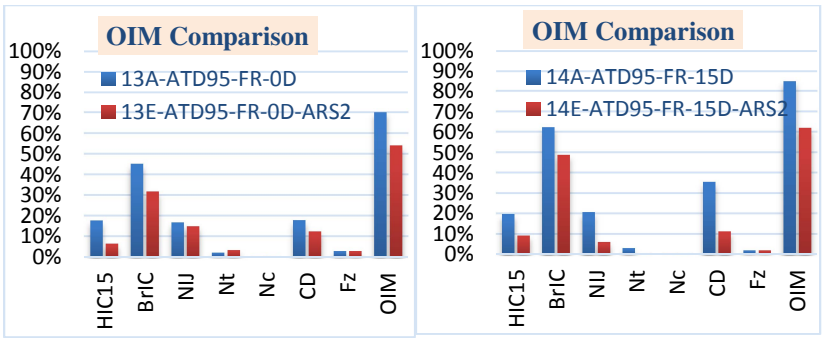

(i) Case 13E vs. 13A (ii) Case 14E vs. 14A

Figure 2. Comparison of the ATD estimated Occupant Injury Measures for the AIS 3+ injury risks between the adaptive restraints (ARS2) and the baseline restraints for the fourteen load cases. Blue bars—the baseline; red bars—the ARS2.

Occupant Injury Measures from HMs

Figure 3 compares the HMs estimated Occupant Injury Measures for the AIS 3+ injury risks between the ARS2 and the baseline restraints for the fourteen load cases. The human body injury measures outputted from the HMs are listed in Table E-2 in Appendix E. For the thirteen out of the fourteen load cases, the human models predicted that the ARS2, obtained from the optimization ATDs cycles, generated the lower OIMs than the baseline restraints. The percentages of the injury measure reduction over the baseline were in the range of 8%-66%. For all the fourteen load cases, there were no case with the baseline restraints, in which the OIM was less than 20%. With the adaptive restraint system, less than 20% of the OIMs estimated from the HMs were observed from five cases.

However, there was one exceptional case (Case 11F: the 95th%ile male human model at the mid-track position at the 0^{o} hard pulse), in which the OIM from the ARS2 was higher than that from the baseline mainly caused by the spike of the HIC number due to the airbag bottoming out. In this case, the "optimized" set of design parameters from the Hybrid-III 95th%ile dummy lead to the soft passenger airbag deployment.

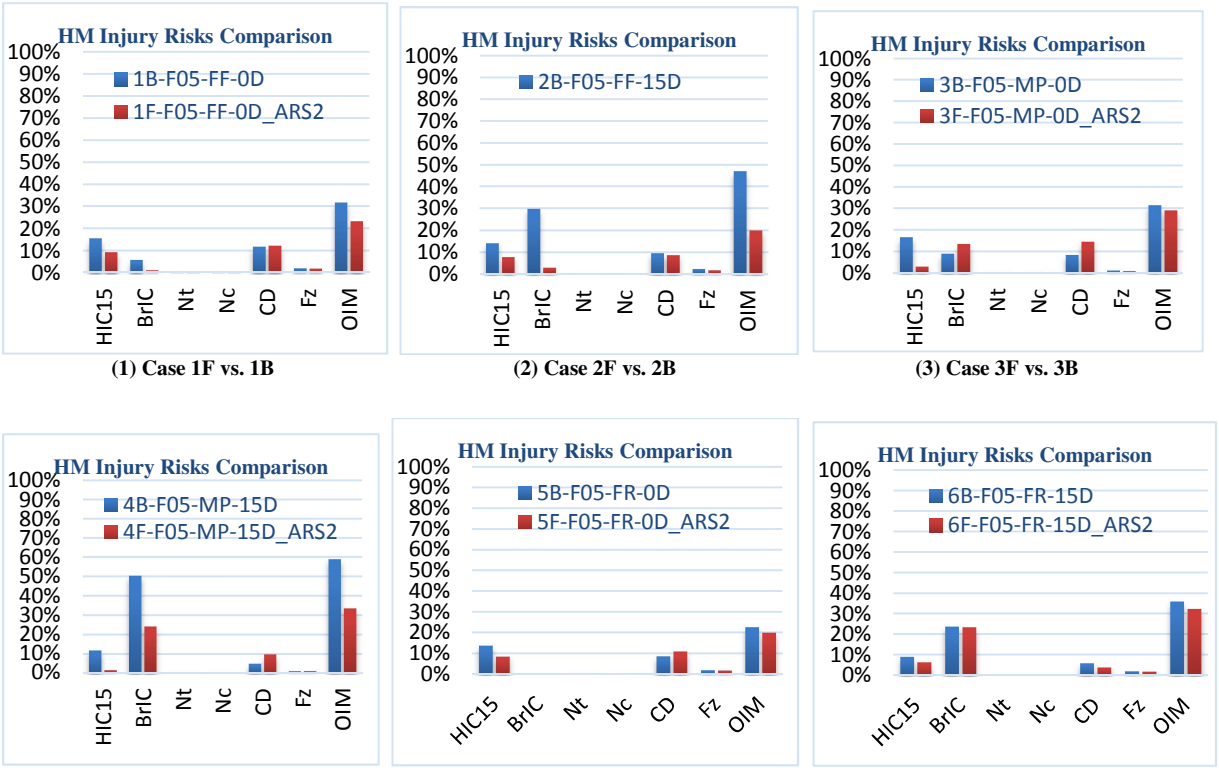

(1) Case 1F vs. 1B (2) Case 2F vs. 2B (3) Case 3F vs. 3B

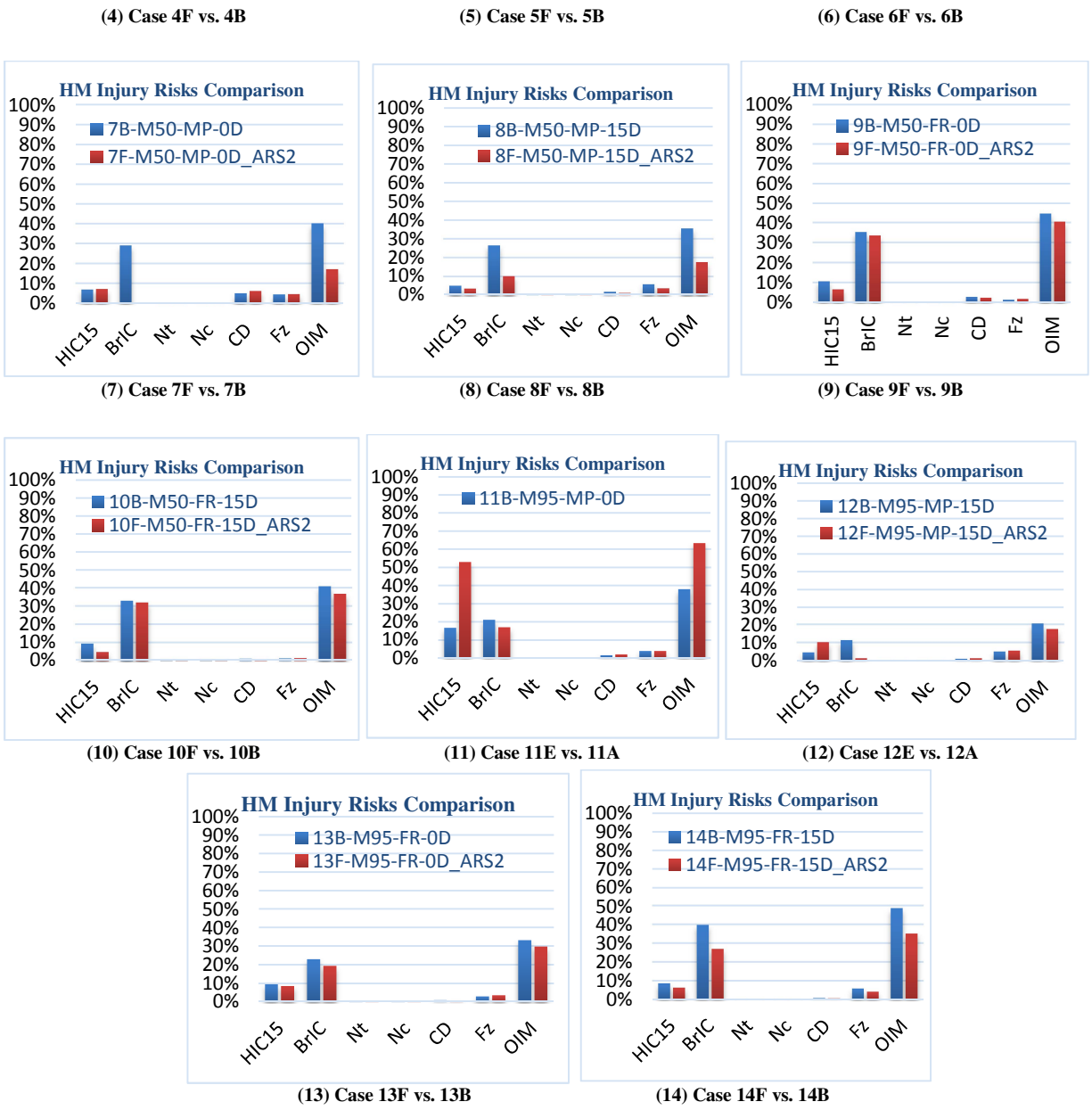

Figure 3. Comparison of the HM predicted Occupant Injury Measures for the AIS 3+ injury risks between the adaptive restraints (ARS2) and the baseline restraints for the fourteen load cases. Blue bars—the baseline; red bars—the ARS2.

It was seen from Figure 3 that the neck injury risk values were very low for all the cases. As shown in Table E-2, there were no outputs of the neck tension and compression forces in some cases for the 5th%ile female dummy, which had zero risk values for these cases. For the rest of cases with the neck forces outputs, however, the neck forces were so low such that the calculated maximum neck injury risk value was only 1.3%. The accuracy of the HM neck occipital forces outputs needs to be further evaluated.

DISCUSSIONS

Differences of the Estimated Occupant Injury Risks: ATDs. vs. HMs

An overview across Figure 2 and 3, we observed differences of the occupant injury risks between those estimated from the ATD and from the HM even at same load case conditions. One observation was that the

ATDs generally estimated higher BrIC based injury risks than the HMs. For some cases, the ATD estimated BrIC based injury risk probabilities were very high (exceeding 80%), while the maximum HM estimated BrIC based injury risk probabilities were less than 50%.

To understand more about the main body regions risks, we compared the predicted OIMs by HMs with the ones estimated by ATDs for the six load cases of the three occupant sizes and seating positions, as depicted in Figure 4. In this analysis, the neck injury risk values were excluded. It was seen that overall the HMs predicted the smaller OIMs than the ATDs. Further review of the four body region injury measures, we observed the lower chest injury risks (CD) estimated from the mid-size and large-size occupant HMs compared to those from the ATDs.

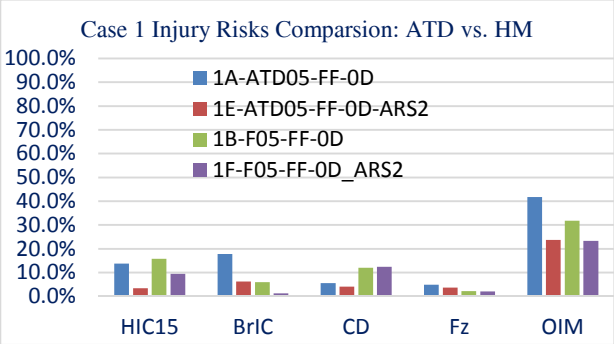

Case 1: the 5th %ile female at full-forward position

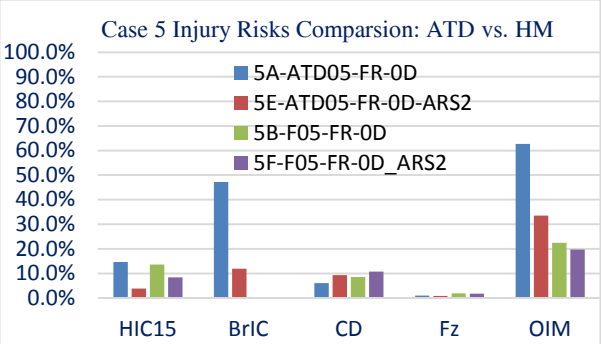

Case 5: the 5th %ile female at full-rearward position

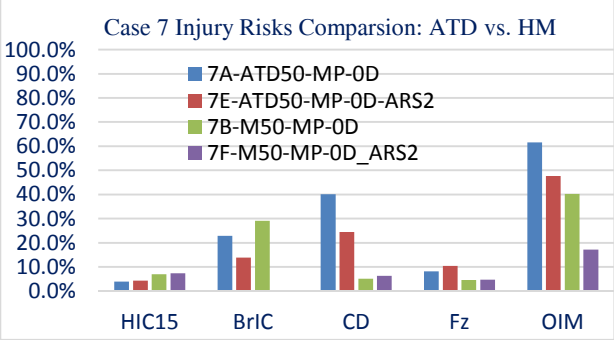

Case 7: the 50th %ile male at mid-track position

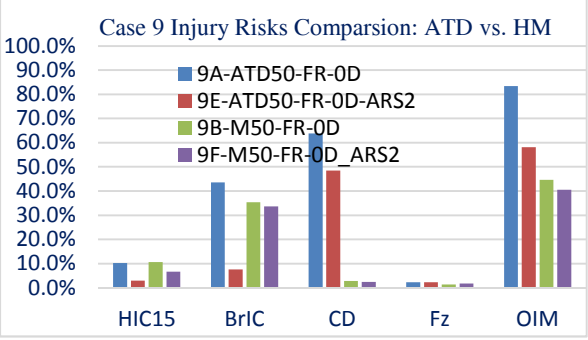

Case 9: the 50th %ile male at full-rearward position

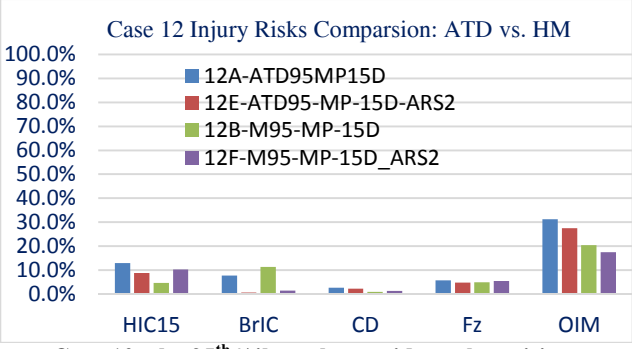

Case 12: the 95th %ile male at mid-track position

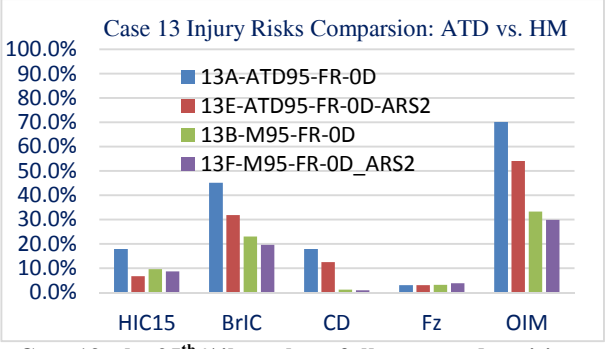

Case 13: the 95th %ile male at full-rearward position

Figure 4. Comparison of the HM predicted Occupant Injury Measures with the ATD estimated ones for the six load cases

Occupant Body Size Effect

We also analyzed the data to better understand the effects of the occupant body sizes and the injury assessment tools. Figure 5 shows the trends of OIMs varying with the occupant sizes, the seating positions (focused on the

Mid-Track and Full-rearward positions), and the crash modes. The data were obtained from the simulations with ATDs and the HMs for the baseline restraints. It was seen that the mid-size and large size males suffered relatively higher OIMs at the left 15° angled hard pulse in general. Another observation was that regardless of the seating positions and the pulse modes the Hybrid-III large sized male dummy generated the lower OIMs than the mid-size THOR dummy, which was confirmed from the ATD sled tests in the AARP. While the large-size male HM predicted the higher OIMs than the mid-sized male at the same full-rearward position at 15° angled hard pulse.

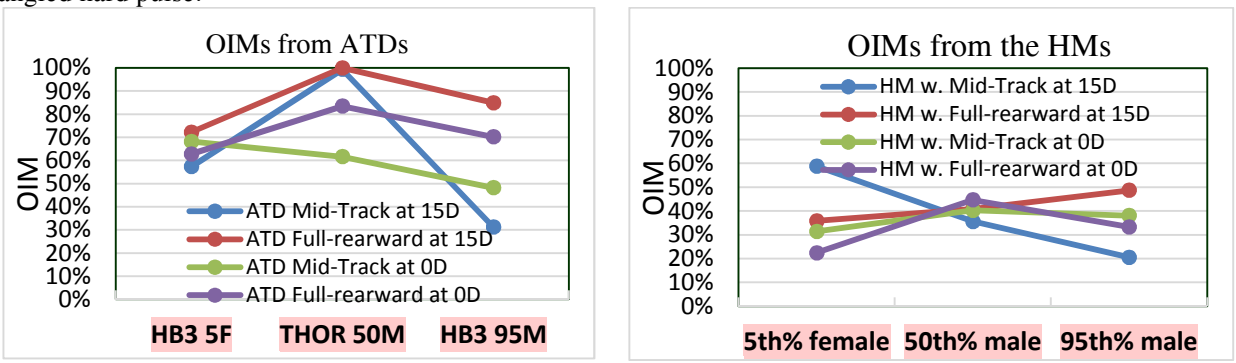

(1) the OIMs estimated from the ATDs **(1) the OIMs estimated from the HMs**

Figure 5. Comparison of the trends of OIMs varying with the occupant sizes, the seating positions, and the crash modes: the ATDs vs. the HMs. All the plotted data related to the baseline restraints.

Limitations of this Study

This study generated a large set of data from hundreds of the sled test simulations using the fifty-six sled system models. Although a portion of the ATD sled test models were directly validated with the real sled tests, the rest of the sled models with ATD or GHBMC Human Body Models were not directly validated since such experimental data does not exist. Nevertheless, this study was performed in multiple steps at large scale to evaluate potential benefits of the new concept design of the adaptive restraint system. The benefits were strictly assessed on the relative basis.

For the first time we deployed three sizes of GHBMC detailed human occupant models in the sled system simulations for evaluation of the adaptive restraint performances. Only those global injury measures that are the same as the ATD injury measures used in the regulation were analyzed in this paper. The other global injury measures for other body regions like the abdomen and lower extremities were processed from the human models, but the data were not included in this analysis. More analysis for those missed body region injuries are in working progress.

As shown in the results section, the outputted neck occipital joint forces were relatively low, for which further validation of the outputs is suggested for the occupant models.

The human models could generate a lot of data for assessing possible tissue level injuries of the occupants. In this paper such data analysis is not included. Considering that the GHBMC human models have been under continuous development, more detailed analysis on the tissue level injuries will be included in the next step studies once the update versions of the GHBMC models with more validations are available.

CONCLUSIONS

The new passenger adaptive restraint system developed from this study showed good benefits of reducing occupant injury risks over the current production restraints for the fourteen load cases considering the three body size occupants at the three seating positions under the two severe frontal crash modes. The occupant injury risks reduction percentages, varying case by case, are 12%-79% estimated with the ATDs and 8%-66% with the HMs.

New methods for evaluation and optimization of the adaptive restraint system designs were exercised using both the ATDs and the HMs of three body sizes. This new restraint evaluation protocol, with further

enhancement for the tools and processes, could be standardized for assessment of future adaptive restraint system designs.

Emerging occupant classification and monitoring systems offer the potential for protection improvement by calibrating the advanced restraint systems to optimize the level of protection for every occupant in the vehicle at different seating position. The future of occupant protection would be a dynamic, situational, intelligent personalized system based on the occupant data collected during normal vehicle usage. A combination of human body modeling tools and advanced occupant sensing would drive reduction in serious injuries caused by motor vehicle crashes.

ACKNOWLEDGEMENTS

Mike Scavnicky, Bernd Cyliax, Ingo Mueller, Torsten Steiner at Joyson Safety Systems made great contributions to AARP activities, from which the selected sled tests data were used for this study. The AARP project was funded by NHTSA Contract #DTNH22-12-C-00266. The authors greatly appreciate the support from NHTSA, especially James Saunders, Stephen Summers, and Dan Parent,

REFERENCES

Cyliax, B., Scavnicky, M., Mueller, I., Zhao, J., and Aoki, H. 2015. "Advanced Adaptive Restraints Program Individualization of Occupant Safety Systems", SAE 2015 Government/Industry Meeting, Washington, DC.

Bose, D., Crandall, J., Untaroiu, C., Maslen, E., "Influence of Pre-collision Occupant Properties on the Injury Response During Frontal Collisions", IRCOBI paper, September 2008.

Bugler, et al., Seattle CIREN Team (Bulger, Dissanaike, Kaufman, Mack), University of Washington, Harborview Injury Prevention and Research Center, " The Effects of Seatback Reclined Positions of Occupants in Motor Vehicles Collisions", CIREN Meeting 2007.

Eppinger, R., et al., 1999, "Development of Improved Injury Criteria for the Assessment of Advanced Automotive Restraint Systems - II", NHTSA

Eppinger, R., et al., 2000, "Supplement: Development of Improved Injury Criteria for the Assessment of Advanced Automotive Restraint Systems - II", NHTSA.

Gaewsky J., "Driver Injury Metric and Risk Variability as a Function of Occupant Position in Real World Motor Vehicle Crashes", Traffic Injury Prevention 16(sup2):S124-S131 · October 2015

Kent, R., Forman, J., et al., 2006, "Whole-body Kinematic and Dynamic Response of Restrained PMHS in Frontal Sled Tests", Stapp Car Crash Journal 50: 299-336.

Kuppa, S., et al., 2001, "Lowe Extremity Injuries and Associated Injury Criteria", 24th ESV Conference, Paper No. 457.

Laituri, T., et al., 2005, "Derivation and Evaluation of a Provisional, Age-Dependent, AIS3+ Thoracic Risk Curve for Belted Adults in Frontal Impacts", SAE World Congress, 2005-01-0297.

Parent, D. et al., 2015, "NHTSA THOR Update", THOR Public Meeting, Washington, DC.

Wang, S. C., et al., " Reference Analytic Morphomics Population (RAMP): A Reference to Measure Occupant Variability for Crash Injury Analysis", *IRC-16-80,* IRCOBI Conference 2016

Takhounts, E., Craig, JC., Moorhouse, K., and McFadden, J., 2013, "Development of Brain injury Criteria (BrIC)", Stapp Car Crash Journal 57: 343-266.

Zhao, J., Katagiri, M., "GHBMC Model Simulations in Frontal and Oblique Sled Tests for Different Body Sizes and Seating Positions", VDI Conference on Human Body Modelling in Automotive Safety, November 28-29, 2017, Waldorf Astoria Berlin, Germany.

Zhao, J., Zhang, N., and Hu J. 2015. "Implementation of THOR FE Model in AARP Project", NHTSA Public Meeting Concerning Test Device for Human Occupant Restraint, Washington, DC.

Appendix-A: The ATD Sled Test Models Correlation

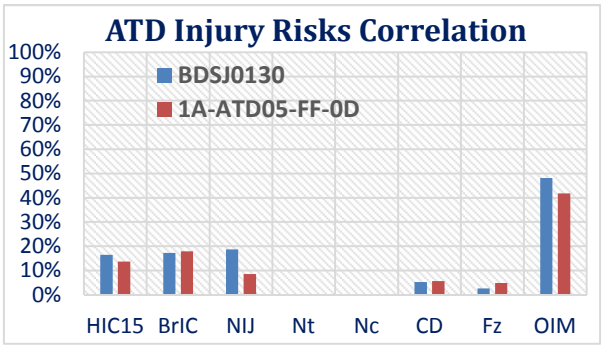

(a) Case 1A-ATD05-FF-0D

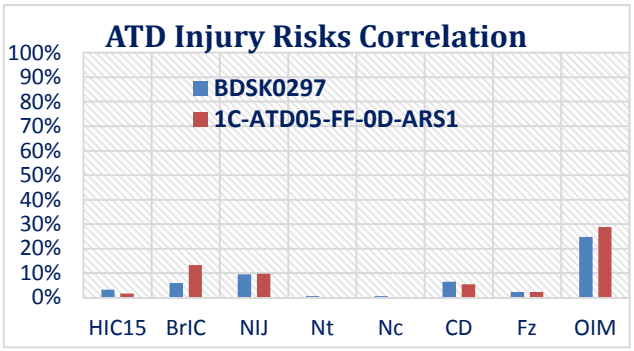

(b) Case 1C-ATD05-FF-0D-ARS1

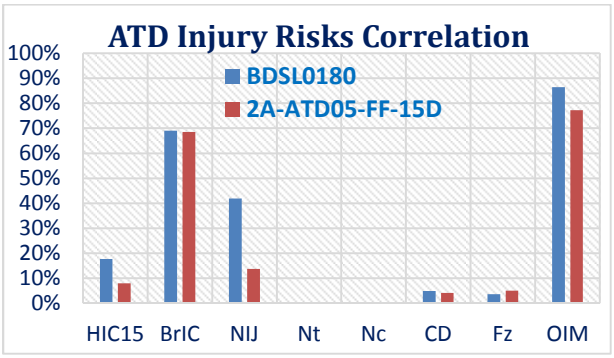

(a) Case 2A-ATD05-FF-15D

(b)

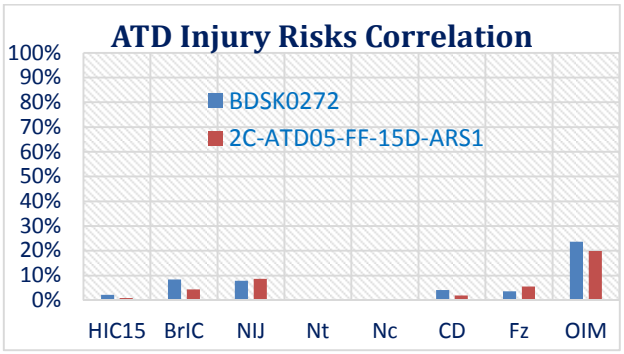

(b) Case 2C-ATD05-FF-15D-ARS1

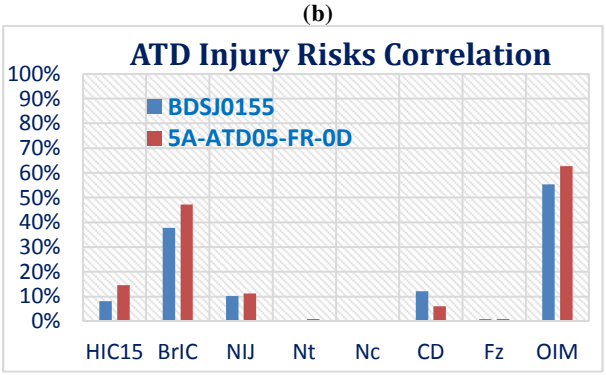

(a) Case 5A-ATD05-FR-0D-B

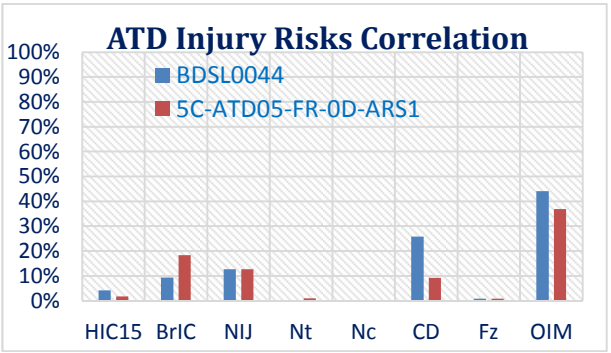

(b) Case 5C-ATD05-FR-0D -ARS1

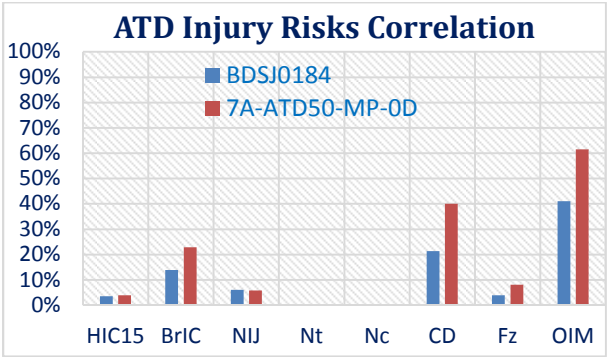

(a) Case 7A-ATD50-FR-0D

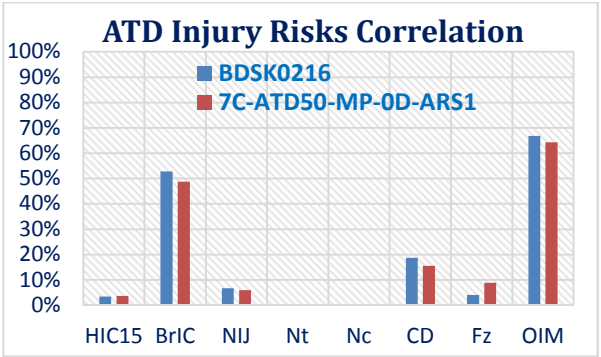

(b) Case 7C-ATD50-FR-0D-ARS1

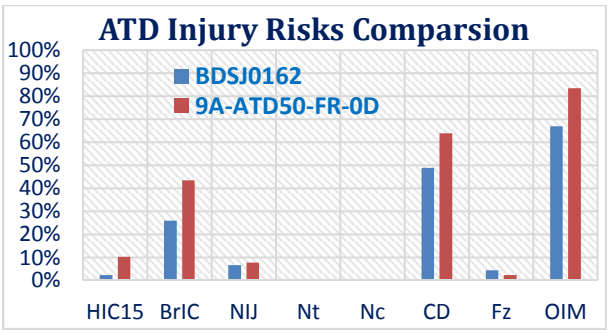

(a) Case 9A-ATD50-FR-0D

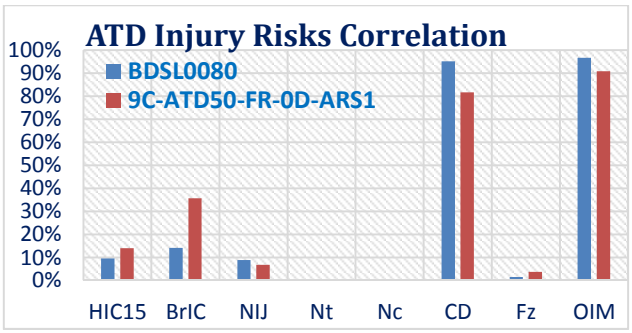

(b) Case 9C-ATD50-FR-0D-ARS1

Figure A-1. Correlation of the injury risks between the predicted from the sled simulations (red) and the calculated from the test measurement data (Blue)

Appendix-B: Additional Technical Info on The Load Case Definitions

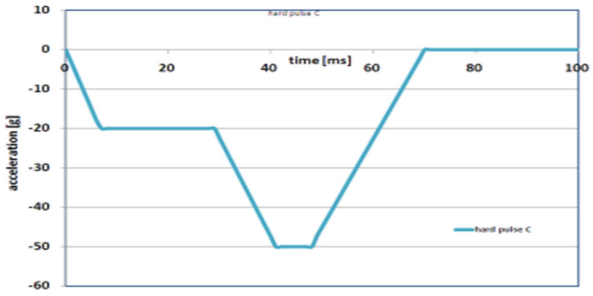

(a) 35mph Hard Pulse 0°

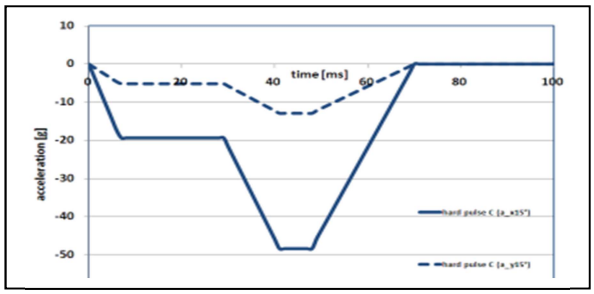

(b) 35mph Hard pulse 15°

Figure B-1. The AARP hard pulses represented a 35mph crash of a sub-compact car used in this study

Table B-1.
The sled test models developed from this study

Seq #	Case No	Case Name	Occ. Model	Pulse Angle	Occ. Size	Seat Position	Restraints
1	1A	ATDF05_FF_0D	HB3-05	0°	5%	Full Forward	Baseline
2	2A	ATDF05_FF_15D	HB3-05	LT-15°	5%	Full Forward	Baseline
3	3A	ATDF05_MP_0D	HB3-05	0°	5%	Mid-Track	Baseline
4	4A	ATDF05_MP_15D	HB3-05	LT-15°	5%	Mid-Track	Baseline
5	5A	ATDF05_FR_0D	HB3-05	0°	5%	Full Rear	Baseline
6	6A	ATDF05_FR_15D	HB3-05	LT-15°	5%	Full Rear	Baseline
7	7A	ATDM50_MP_0D	THOR-50M	0°	50%	Mid-Track	Baseline
8	8A	ATDM50_MP_15D	THOR-50M	LT-15°	50%	Mid-Track	Baseline
9	9A	ATDM50_FR_0D	THOR-50M	0°	50%	Full Rear	Baseline
10	10A	ATDM50_FR_15D	THOR-50M	LT-15°	50%	Full Rear	Baseline
11	11A	ATDM95_MP_0D	HB3-95	0°	95%	Mid-Track	Baseline
12	12A	ATDM95_MP_15D	HB3-95	LT-15°	95%	Mid-Track	Baseline
13	13A	ATDM95_FR_0D	HB3-95	0°	95%	Full Rear	Baseline
14	14A	ATDM95_FR_15D	HB3-95	LT-15°	95%	Full Rear	Baseline
15	1B	F05_FF_0D	GHBMC F05-O 3.1	0°	5%	Full Forward	Baseline

16	2B	F05_FF_15D	GHBMC F05-O 3.1	LT-15°	5%	Full Forward	Baseline
17	3B	F05_MP_0D	GHBMC F05-O 3.1	0°	5%	Mid-Track	Baseline
18	4B	F05_MP_15D	GHBMC F05-O 3.1	LT-15°	5%	Mid-Track	Baseline
19	5B	F05_FR_0D	GHBMC F05-O 3.1	0°	5%	Full Rear	Baseline
20	6B	F05_FR_15D	GHBMC F05-O 3.1	LT-15°	5%	Full Rear	Baseline
21	7B	M50_MP_0D	GHBMC M50-O v4.5	0°	50%	Mid-Track	Baseline
22	8B	M50_MP_15D	GHBMC M50-O v4.5	LT-15°	50%	Mid-Track	Baseline
23	9B	M50_FR_0D	GHBMC M50-O v4.5	0°	50%	Full Rear	Baseline
24	10B	M50_FR_15D	GHBMC M50-O v4.5	LT-15°	50%	Full Rear	Baseline
25	11B	M95_MP_0D	GHBMC M95-O v1.3	0°	95%	Mid-Track	Baseline
26	12B	M95_MP_15D	GHBMC M95-O v1.3	LT-15°	95%	Mid-Track	Baseline
27	13B	M95_FR_0D	GHBMC M95-O v1.3	0°	95%	Full Rear	Baseline
28	14B	M95_FR_15D	GHBMC M95-O v1.3	LT-15°	95%	Full Rear	Baseline
29	1E	ATDF05_FF_0D	HB3-05	0°	5%	Full Forward	ARS2
30	2E	ATDF05_FF_15D	HB3-05	LT-15°	5%	Full Forward	ARS2
31	3E	ATDF05_MP_0D	HB3-05	0°	5%	Mid-Track	ARS2
32	4E	ATDF05_MP_15D	HB3-05	LT-15°	5%	Mid-Track	ARS2
33	5E	ATDF05_FR_0D	HB3-05	0°	5%	Full Rear	ARS2
34	6E	ATDF05_FR_15D	HB3-05	LT-15°	5%	Full Rear	ARS2
35	7E	ATDM50_MP_0D	THOR-50M	0°	50%	Mid-Track	ARS2
36	8E	ATDM50_MP_15D	THOR-50M	LT-15°	50%	Mid-Track	ARS2
37	9E	ATDM50_FR_0D	THOR-50M	0°	50%	Full Rear	ARS2
38	10E	ATDM50_FR_15D	THOR-50M	LT-15°	50%	Full Rear	ARS2
39	11E	ATDM95_MP_0D	HB3-95	0°	95%	Mid-Track	ARS2
40	12E	ATDM95_MP_15D	HB3-95	LT-15°	95%	Mid-Track	ARS2
41	13E	ATDM95_FR_0D	HB3-95	0°	95%	Full Rear	ARS2
42	14E	ATDM95_FR_15D	HB3-95	LT-15°	95%	Full Rear	ARS2
43	1F	F05_FF_0D	GHBMC F05-O 3.1	0°	5%	Full Forward	ARS2
44	2F	F05_FF_15D	GHBMC F05-O 3.1	LT-15°	5%	Full Forward	ARS2
45	3F	F05_MP_0D	GHBMC F05-O 3.1	0°	5%	Mid-Track	ARS2
46	4F	F05_MP_15D	GHBMC F05-O 3.1	LT-15°	5%	Mid-Track	ARS2
47	5F	F05_FR_0D	GHBMC F05-O 3.1	0°	5%	Full Rear	ARS2
48	6F	F05_FR_15D	GHBMC F05-O 3.1	LT-15°	5%	Full Rear	ARS2
49	7F	M50_MP_0D	GHBMC M50-O v4.5	0°	50%	Mid-Track	ARS2
50	8F	M50_MP_15D	GHBMC M50-O v4.5	LT-15°	50%	Mid-Track	ARS2
51	9F	M50_FR_0D	GHBMC M50-O v4.5	0°	50%	Full Rear	ARS2
52	10F	M50_FR_15D	GHBMC M50-O v4.5	LT-15°	50%	Full Rear	ARS2
53	11F	M95_MP_0D	GHBMC M95-O v1.3	0°	95%	Mid-Track	ARS2
54	12F	M95_MP_15D	GHBMC M95-O v1.3	LT-15°	95%	Mid-Track	ARS2
55	13F	M95_FR_0D	GHBMC M95-O v1.3	0°	95%	Full Rear	ARS2
56	14F	M95_FR_15D	GHBMC M95-O v1.3	LT-15°	95%	Full Rear	ARS2

Appendix-C: The ARS2 Restraint System Parameters

Table C-1.
ARS2 system components and design parameters defined in this study

Component	NO.	Parameter	Classification
Passenger Airbag (PAB)	1	Inflator TTF (ms)	P
	2	Fixed Vent size (mm)	N
	3	Tether Length	N
	4	Active Vent (AV) size (mm)	N
	5	AV Opening Time (ms)	P
	6	Volume Switch Time (ms)	P
Knee Airbag (KAB)	7	Inflator TTF (ms)	P
	8	Tether Length	N
	9	AV Size (mm)	N
	10	AV Opening Time (ms)	P
	11	Volume Swtich Time (ms)	P
Seatbelt (SB)	12	Retractor & Sho PT TTFs (ms)	P
	13	1st Load Limiter (KN)	N
	14	2nd Load Limiter (KN)	N
	15	Load Limiter Switch Time (ms)	P
	16	Lap PT TTF (ms)	P
RH Curtain Airbag (CAB)	17	Inflator TTF (ms)	P

- P—Programmable; N—Non-programmable

Appendix-D: Injury Risk Functions for the ATDs and HMs

The risk injury functions for each measure as well as a combined injury probability for the whole body were same as those defined in new US NCAP NPRM [US NCAP NPRM, 2016], summarized in Table E-1. The function of Nt and Nc for Hybrid III 95th%ile male was scaled from that for 50th%ile male based on the scaling factor reported in Eppinger et al., 1999. The injury risk functions for the human models were summarized in Table E-2.

Table D-1.
The injury risk functions for the ATDs

	Hybrid III 5th%ile female	THOR 50th%ile male	Hybrid III 95th%ile male	Function	Reference
HIC	✓	✓	✓	$P(AIS\,3+) = \emptyset\left[\frac{\ln(HIC) - 7.45231}{0.73998}\right]$	US NCAP
BrIC	✓	✓	✓	$P(AIS\,3+) = 1 - e^{-\left(\frac{BrIC-0.523}{0.531}\right)^{1.8}}$	US NCAP

Nij	✓	✓	✓	$P(AIS\,3+) = \frac{1}{1+e^{(3.227-1.969*Nij)}}$	US NCAP
Nt, Nc	✓			$P(AIS\,3+) = \frac{1}{1+e^{(10.958-3.77*Nt\ or\ Nc)}}$	US NCAP
		✓		$P(AIS\,3+) = \frac{1}{1+e^{(10.975-2.375*Nt\ or\ Nc)}}$	US NCAP
			✓	$P(AIS\,3+) = \frac{1}{1+e^{(10.975-1.966*Nt\ or\ Nc)}}$	US NCAP*
CD	✓			$P(AIS\,3+) = \frac{1}{1+e^{(10.5456-1.7212*CD^{0.4612})}}$	US NCAP
		✓		$P(AIS\,3+) = 1-e^{-\left(\frac{CD}{e^{4.4853-0.0113}}\right)^{5.03896}}$	US NCAP
			✓	$P(AIS\,3+) = \frac{1}{1+e^{(10.5456-1.4956*CD^{0.4612})}}$	FMVSS 208
Femur Fz	✓			$P(AIS\,3+) = \frac{1}{1+e^{(4.9795-0.478*Fz)}}$	US NCAP
		✓		$P(AIS\,3+) = \frac{1}{1+e^{(4.9795-0.326*Fz)}}$	US NCAP
			✓	$P(AIS\,3+) = \frac{1}{1+e^{(4.9795-0.257*Fz)}}$	FMVSS 208

Table D-2.
The injury risk functions for the HMs

	HM 5th%ile female	HM 50th%ile male	HM 95th%ile male	Function	Reference
HIC	✓	✓	✓	$P(AIS\,3+) = \emptyset\left[\frac{\ln(HIC)-7.45231}{0.73998}\right]$	Eppinger, 2000
BrIC	✓	✓	✓	$P(AIS\,3+) = 1-e^{-\left(\frac{BrIC-0.523}{0.531}\right)^{1.8}}$	Takhounts, 2013
Nt, Nc	✓			$P(AIS\,3+) = \frac{1}{1+e^{(10.958-3.77*Nt\ or\ Nc)}}$	Eppinger, 1999
		✓		$P(AIS\,3+) = \frac{1}{1+e^{(10.975-2.375*Nt\ or\ Nc)}}$	
			✓	$P(AIS\,3+) = \frac{1}{1+e^{(10.975-1.966*Nt\ or\ Nc)}}$	
CD	✓	✓	✓	$P(AIS\,3+) = \frac{1}{1+e^{(12.957-0.05861*65YO-26.9*CD\%)}}$	Laituri, 2005
Femur Fz	✓			$P(AIS\,3+) = \frac{1}{1+e^{(4.9795-0.478*Fz)}}$	Kuppa, 2001
		✓		$P(AIS\,3+) = \frac{1}{1+e^{(4.9795-0.326*Fz)}}$	
			✓	$P(AIS\,3+) = \frac{1}{1+e^{(4.9795-0.257*Fz)}}$	

Appendix-E: Injury Measures from the ATDs

Table E-1.
The injury measures from the baseline restraints A- class ATD sled test models and the ARS2 E- class ATD sled models

Body Region	Head		Neck			Thorax					KTH	
Injury Measure /Case	HIC 15	BrIC	NIJ	Neck Tension (kN)	Neck Compression (kN)	Chest G 3ms (G)	Chest Def. UR (mm)	Chest Def. UL (mm)	Chest Def. LR (mm)	Chest Def. LL (mm)	Femur Load - Right (kN)	Femur Load - Left (kN)
1A-ATD05-FF-0D	767.5	0.785	0.44	1.028	0.331	58.3	25.9	25.9	25.9	25.9	3.480	4.197
1E-ATD05-FF-0D-ARS2	446.6	0.664	0.46	1.143	0.379	44.1	23.5	23.5	23.5	23.5	3.350	3.560
2A-ATD05-FF-15D	608.6	1.225	0.70	1.409	0.103	60.5	23.5	23.5	23.5	23.5	3.213	4.276

2E-ATD05-FF-15D-ARS2	403.9	0.482	0.46	1.224	0.080	44.0	19.6	19.6	19.6	19.6	2.756	3.498
3A-ATD05-MP-0D	685.9	1.126	0.51	0.768	0.201	56.6	21.7	21.7	21.7	21.7	1.690	1.257
3E-ATD05-MP-0D-ARS2	365.9	0.789	0.43	1.610	0.128	46.7	26.8	26.8	26.8	26.8	0.558	0.551
4A-ATD05-MP-15D	912.1	0.974	0.39	0.707	0.461	58.8	17.7	17.7	17.7	17.7	1.332	1.218
4E-ATD05-MP-15D-ARS2	331.6	0.663	0.52	1.391	0.136	42.2	22.1	22.1	22.1	22.1	0.458	0.560
5A-ATD05-FR-0D	790.0	1.027	0.59	1.656	0.848	46.5	26.5	26.5	26.5	26.5	0.619	0.399
5E-ATD05-FR-0D-ARS2	463.0	0.728	0.66	1.597	0.544	40.1	30.0	30.0	30.0	30.0	0.398	0.558
6A-ATD05-FR-15D	1129.1	1.083	0.77	1.946	0.306	72.1	0.3	0.3	0.3	0.3	0.920	0.579
6E-ATD05-FR-15D-ARS2	470.8	0.933	0.64	1.613	0.115	44.2	22.5	22.5	22.5	22.5	0.216	0.559
7A-ATD50-MP-0D_B	470.5	0.829	0.23	1.385	0.415	45.8	34.8	38.0	9.2	46.7	6.937	7.826
7E-ATD50-MP-0D-ARS2	481.9	0.747	0.27	1.411	0.595	50.8	0.8	35.6	8.6	41.5	8.685	7.419
8A-ATD50-MP-15D-B	589.8	1.433	0.25	1.489	0.911	52.1	30.6	6.5	30.6	66.3	5.811	7.036
8E-ATD50-MP-15D-ARS2	412.5	0.814	0.32	1.980	0.306	47.2	0.5	35.6	6.9	40.0	8.778	6.559
9A-ATD50-FR-0D-B	674.9	0.997	0.38	1.764	0.201	90.3	1.2	30.0	12.8	53.5	3.218	3.669
9E-ATD50-FR-0D-ARS2	426.2	0.680	0.36	1.635	0.030	51.1	1.1	28.5	14.5	49.1	2.640	3.799
10A-ATD50-FR-15D-B	756.5	1.288	1.30	1.219	1.461	67.6	49.8	11.9	49.8	59.3	3.028	2.025
10E-ATD50-FR-15D-ARS2	253.8	0.942	0.30	1.678	0.029	45.2	1.2	18.0	12.0	36.3	2.884	2.453
11A-ATD95-MP-0D	797.9	0.872	0.30	2.062	1.390	49.5	30.4	30.4	30.4	30.4	8.705	7.283
11E-ATD95-MP-0D-ARS2	598.5	0.832	0.34	3.538	1.219	41.9	28.5	28.5	28.5	28.5	8.808	8.310
12A-ATD95MP15D	746.4	0.683	0.30	2.242	1.296	57.8	27.8	27.8	27.8	27.8	8.525	7.304
12E-ATD95-MP-15D-ARS2	633.5	0.561	0.72	3.353	1.436	56.5	26.3	26.3	26.3	26.3	7.433	7.699
13A-ATD95-FR-0D	870.9	1.010	0.83	3.666	1.743	66.4	49.2	49.2	49.2	49.2	4.120	5.861
13E-ATD95-FR-0D-ARS2	566.5	0.903	0.76	3.894	1.891	51.1	44.4	44.4	44.4	44.4	3.704	5.774
14A-ATD95-FR-15D	918.4	1.162	0.96	3.821	0.545	67.8	60.9	60.9	60.9	60.9	4.203	3.871
14E-ATD95-FR-15D-ARS2	646.3	1.040	0.25	1.287	0.035	68.7	43.2	43.2	43.2	43.2	4.299	4.242

Table E-2.
The injury measures from the baseline restraints B- class HM sled test models and the ARS2 F- class HM sled models

Body Region	Head		Neck		Thorax						KTH	
Injury Measure	HIC 15	BrIC	Neck Tension (kN)	Neck Compression (kN)	Chest G 3ms (G)	Chest Def. UR (mm)	Chest Def. UL (mm)	Chest Def. LR (mm)	Chest Def. LL (mm)	Chest Def-Sternum (mm)	Femur Load - Right/kN (FzR)	Femur Load - Left/kN (FzL)
1B-F05-FF-0D	818.9	0.66	0.36	0.023	83.1	57.6	57.8	56.4	53.4	53.0	2.510	2.175

1F-F05-FF-0D_ARS2	652.0	0.58	0.30	0.037	66.5	54.8	54.5	63.2	49.3	53.3	2.385	2.323
2B-F05-FF-15D	779.3	0.89	NA	NA	80.6	54.9	53.6	11.1	33.7	51.1	2.731	2.164
2F-F05-FF-15D_ARS2	551.3	0.67	0.048	0.052	72.4	51.5	50.9	50.9	44.9	50.4	2.078	2.024
3B-F05-MP-0D	842.8	0.70	NA	NA	64.5	51.9	48.6	70.7	55.4	50.0	1.233	0.809
3F-F05-MP-0D_ARS2	432.0	0.75	NA	NA	56.0	56.3	49.5	55.6	42.3	54.8	0.574	0.744
4B-F05-MP-15D	715.9	1.05	NA	NA	79.5	46.6	41.2	46.4	28.3	45.5	0.987	0.918
4F-F05-MP-15D_ARS2	352.4	0.84	NA	NA	65.2	52.8	46.5	41.0	24.4	51.3	1.165	0.906
5B-F05-FR-0D	764.5	0.52	NA	NA	70.3	55.7	46.6	24.0	39.1	50.0	2.128	1.508
5F-F05-FR-0D_ARS2	599.7	0.40	0.132	0.039	57.8	58.2	47.7	11.9	39.6	52.1	2.040	1.401
6B-F05-FR-15D	638.0	0.84	NA	NA	242.8	52.2	44.9	27.8	37.5	47.0	2.232	1.434
6F-F05-FR-15D_ARS2	556.7	0.83	NA	NA	254.4	48.2	40.9	24.5	34.4	43.4	2.112	1.393
7B-M50-MP-0D	575.7	0.88	0.56	0.012	68.7	50.6	56.7	40.2	48.3	48.5	5.924	5.388
7F-M50-MP-0D_ARS2	588.1	0.51	0.91	0.090	65.5	51.2	59.1	36.5	50.7	50.4	6.029	5.039
7B-M50OS-MP-0D	397.7	0.79	15.00	3.292	68.8	45.3	61.4	9.8	57.2	54.9	5.239	4.992
7F-M50OS-MP-0D_ARS2	394.3	0.98	15.44	34.074	69.4	40.6	63.3	9.7	59.9	54.9	5.061	3.877
8B-M50-MP-15D	511.1	0.86	0.70	0.035	65.6	42.1	46.7	21.9	39.5	40.2	3.997	6.761
8F-M50-MP-15D_ARS2	452.9	0.71	0.87	0.024	84.3	36.8	44.0	29.3	35.1	37.0	5.286	4.980
9B-M50-FR-0D	685.6	0.93	1.11	0.002	165.4	45.1	58.7	20.1	69.4	43.5	1.646	2.028
9F-M50-FR-0D_ARS2	565.4	0.92	1.32	0.001	158.6	41.9	56.0	24.8	69.2	42.1	2.928	2.471
10B-M50-FR-15D	652.4	0.91	1.19	0.002	87.5	42.3	48.4	40.4	63.1	37.0	1.709	2.253
10F-M50-FR-15D_ARS2	508.1	0.90	1.11	0.199	160.1	34.3	41.8	14.3	54.7	31.5	2.433	1.570
11B-M95-MP-0D	845.7	0.81	0.82	0.065	74.0	63.0	52.1	17.7	54.7	41.0	6.285	7.030
11F-M95-MP-0D_ARS2	1823.9	0.778	1.004	0.057	79.0	63.7	50.6	9.5	55.3	42.9	5.536	6.928
12B-M95-MP-15D	495.4	0.72	0.823	0.069	67.5	55.5	44.3	13.2	47.8	36.6	5.500	7.908
12F-M95-MP-15D_ARS2	674.4	0.584	0.931	0.059	82.9	57.2	44.1	29.1	49.9	39.0	5.134	8.314
13B-M95-FR-0D	656.7	0.83	1.33	0.028	79.9	64.5	55.7	9.6	80.0	37.7	4.200	5.906
13F-M95-FR-0D_ARS2	628.9	0.80	1.27	0.018	79.8	61.8	52.3	38.3	73.2	35.8	2.904	6.735
14B-M95-FR-15D	631.2	0.97	1.29	0.025	127.3	57.1	47.5	55.0	68.9	34.8	2.995	8.641
14F-M95-FR-15D_ARS2	560.1	0.86	1.16	0.015	91.6	53.0	43.4	60.4	60.2	34.0	2.425	7.250